Effect of plankton composition shifts in the North Atlantic on atmospheric pCO2

Amber Boot[1], Anna von der Heydt[2], and Henk A. Dijkstra[3]

[1]Institute for Marine and Atmospheric Research Utrecht
[2]Universiteit Utrecht, Utrecht
[3]Institute for Marine and Atmospheric research Utrecht

September 26, 2023

Abstract

Marine carbon cycle processes are important for taking up atmospheric CO2 thereby reducing climate change. Biological production is an important pathway of carbon from the surface to the deep ocean where it is stored for thousands of years. Climate change can interact with marine ecosystems via changes in the ocean stratification and ocean circulation. In this study we use the Community Earth System Model version 2 (CESM2) results to assess the effect of a changing climate on biological production and plankton composition in the high latitude North Atlantic Ocean. We find a shift in plankton type dominance from diatoms to small phytoplankton which reduces net primary and export productivity. Using a conceptual carbon-cycle model forced with the CESM2 results, we give a rough estimate of a positive plankton composition-atmospheric CO2 feedback of approximately 60 GtCO2/K warming in the North Atlantic which affects the 1.5K and 2.0K warming safe carbon budgets.

Effect of plankton composition shifts in the North Atlantic on atmospheric pCO_2

A. Boot[1], A. S. von der Heydt[1,2], and H. A. Dijkstra[1,2]

[1]Institute for Marine and Atmospheric research Utrecht, Department of Physics,Utrecht University, Utrecht, the Netherlands
[2]Center for Complex Systems Studies, Utrecht University, Utrecht, the Netherlands

Key Points:

- Biological production decreases significantly in the high latitude North Atlantic in CESM2 under the SSP5-8.5 scenario.
- Plankton type dominance shifts from diatoms to small phytoplankton.
- A positive feedback loop is diagnosed where changes in the physical system decrease biological production, reducing oceanic uptake of CO_2.

Corresponding author: Amber Boot, `d.boot@uu.nl`

Abstract

Marine carbon cycle processes are important for taking up atmospheric CO_2 thereby reducing climate change. Biological production is an important pathway of carbon from the surface to the deep ocean where it is stored for thousands of years. Climate change can interact with marine ecosystems via changes in the ocean stratification and ocean circulation. In this study we use the Community Earth System Model version 2 (CESM2) results to assess the effect of a changing climate on biological production and plankton composition in the high latitude North Atlantic Ocean. We find a shift in plankton type dominance from diatoms to small phytoplankton which reduces net primary and export productivity. Using a conceptual carbon-cycle model forced with the CESM2 results, we give a rough estimate of a positive plankton composition-atmospheric CO_2 feedback of approximately 60 $GtCO_2$/K warming in the North Atlantic which affects the 1.5 K and 2.0 K warming safe carbon budgets.

Plain Language Summary

The marine carbon cycle is important for taking up carbon from the atmosphere and thereby lowering atmospheric CO_2 concentrations. One of the ways the marine carbon cycle transports carbon from the surface to the deep ocean is biological production. Once in the deep ocean, carbon can be stored for thousands of years. Biological production is dependent on environmental conditions such as nutrient availability and ocean temperature, which can be affected by increasing atmospheric CO_2 concentrations. This can lead to a positive (negative) feedback loop, where increasing CO_2 concentration decrease (increase) biological production which in turn decreases (increases) uptake of CO_2 by the ocean, effectively increasing (decreasing) atmospheric CO_2 concentrations. Here, we find in an Earth System Model that under a high emission scenario, biological production decreases significantly in the high latitude North Atlantic Ocean which is primarily the result of a shift in dominant phytoplankton type in this region. Larger diatoms, which are relatively efficient in exporting carbon, are replaced by small phytoplankton which are less efficient. By using a conceptual carbon cycle model, we identify a positive feedback loop where the decrease in biological production increases atmospheric CO_2 by approximately 60 $GtCO_2$ per degree warming.

1 Introduction

To avoid tipping behavior in the Earth system, it is important to keep warming of our planet to a maximum of 1.5 to 2°C (Lenton et al., 2019). Policymakers need to know how much carbon we can still emit before we exceed this warming. However, estimates of this safe carbon budget are difficult and subject to large uncertainties because the Earth system has many processes and feedbacks that are not completely understood yet (Matthews et al., 2021).

The marine carbon pumps (physical, biological and carbonate) are currently responsible for taking up 25-40 percent of anthropogenic carbon (Sabine et al., 2004; DeVries et al., 2017). It is estimated that biological production in the ocean exports approximately 11 GtC yr^{-1} to the deep ocean (Sanders et al., 2014) and that without this export, atmospheric pCO_2 values would be 200-400 ppm higher (Ito & Follows, 2005; Henson et al., 2022). This export production (EP) is dependent on the net primary productivity (NPP). It also depends on plankton composition, since different plankton species have different remineralization depths (Morán et al., 2010; Li et al., 2009; Marinov et al., 2013).

Both EP and NPP are strongly dependent on temperature, ocean circulation, stratification and nutrient input (Doney et al., 2011) which can all affect plankton composition. This is important because changes in plankton composition can transfer through

the food web affecting fish and mammals (Richardson & Schoeman, 2004; Beaugrand, 2009) which can affect fishery yields. Furthermore, plankton composition also affects EP which indirectly influences the air-sea gas exchange of CO_2 that could result in a positive feedback loop under climate change (Cabré et al., 2015). In such a feedback higher CO_2 levels change plankton composition, reducing EP and thus the uptake of CO_2 by the ocean. Finally, a changing plankton composition is one of the hypotheses suggested to explain (part of) the atmospheric pCO_2 (80-100 ppm) variations in the Pleistocene glacial-interglacial cycles (Archer & Maier-Reimer, 1994; Kohfeld et al., 2005), showing the potential of this feedback to affect the climate.

Though climate change is likely to affect plankton stocks, the extent is still uncertain (Osman et al., 2019). Expected effects of global warming are changes in NPP (Behrenfeld et al., 2006), reduced nutrient concentrations in the surface ocean due to stronger stratification (Bopp et al., 2001, 2005; Fu et al., 2016), and plankton composition changes, the latter also due to changing co-limitation of light and nutrients (Marinov et al., 2013; C. M. Moore et al., 2013). Furthermore, on longer timescales, severe nutrient trapping in the Southern Ocean is possible, which reduces biological production over most of the ocean (J. K. Moore et al., 2018). However, uncertainties remain in most (model) studies. This is because the complex timing of blooms are difficult to simulate in highly seasonal regions such as the high latitudes (Martinez et al., 2011), and also because ecosystem models that have more extensive plankton dynamics show larger community composition shifts with climate change (Dutkiewicz et al., 2013; Fu et al., 2016). Comparing CMIP6 models with CMIP5 models, we see an increase in intermodel spread in both NPP and EP (Kwiatkowski et al., 2020; Tagliabue et al., 2021; Henson et al., 2022), highlighting the complexity of the system.

One of the regions that is projected to be affected significantly by climate change is the North Atlantic, a region where biological processes are known to be important for gas exchange of CO_2 (Bennington et al., 2009). Observational studies suggest that plankton composition shifts are already occurring in this region (Hilligsøe et al., 2011; Rivero-Calle et al., 2015). Model simulations under high emission scenarios project that the future North Atlantic will have relatively low warming rates, relatively high acidification rates and a (medium to large) decrease of subsurface oxygen (Bopp et al., 2013). In addition, the stratification and ocean circulation are projected to change, such as a decrease in the strength of the Atlantic Meridional Overturning Circulation (AMOC), which could possibly result in a collapse of plankton stocks in the North Atlantic (Schmittner, 2005). These projected changes would lead to large decreases of NPP and EP (Steinacher et al., 2010; Bopp et al., 2013).

The main novel aspect of this study is to provide an estimate of the plankton composition-atmospheric pCO_2 feedback (Cabré et al., 2015) using climate model simulations for a high emission scenario (SSP5-8.5). We aim to answer the following questions: How does biological production respond to higher pCO_2 levels? Does this lead to a positive or a negative feedback on atmospheric CO_2? And lastly, what does this imply for the safe carbon budget? To investigate these issues we have used two models, the Community Earth System Model v2 (CESM2) and the Simple Carbon Project Model v1.0 (SCP-M) as described in Section 2. Results are shown in Section 3 and are summarized and discussed in Section 4.

2 Method

We analyse output from the Community Earth System Model v2 (CESM2, Danabasoglu et al. (2020)) simulations as used in the Coupled Model Intercomparison Project 6 (CMIP6, Eyring et al. (2016)). This model includes the CAM6 atmospheric model, the CLM land model, the CICE sea-ice model, the POP2 ocean circulation model, and the MARBL ocean biogeochemistry model. Both POP2 (Smith et al., 2010) and MARBL (Long et al., 2021)

are run on a displaced Greenland pole grid at a nominal 1° horizontal resolution, with 60 non-equidistant vertical levels. In MARBL, several elemental cycles, three explicit phytoplankton functional groups (small phytoplankton, diatoms, and diazotrophs), one implicit phytoplankton group (calcifiers), and one zooplankton group are simulated. We analyse output of a single member CESM2 simulation (Danabasoglu, 2019) which is driven by greenhouse gas emissions according to the SSP5-8.5 scenario (B. C. O'Neill et al., 2020; Green et al., 2021). Since it is an emission driven case, atmospheric pCO_2 is affected by feedbacks from the land and ocean reservoirs of carbon. The simulation period is from 2015-2101 and analysis results in section 3 are based on monthly and yearly mean data.

Generally, CESM2 is one of the better performing Earth System Models when ocean biogeochemistry is considered globally (Séférian et al., 2020). MARBL, however, has some biases due to deficiencies in the ocean circulation model (POP2). In particular, the too sluggish deep ocean circulation in POP2 causes nutrient trapping in the deep North Pacific Ocean. In MARBL, this results in low abundances of oxygen throughout the deep Pacific Ocean, which causes organic matter to be remineralized via nitrogen, negatively affecting the quality of the nitrogen cycle simulation. This large bias was fixed by adjusting the stoichiometric ratios of organic matter in the Pacific Ocean so less oxygen is consumed by organic matter remineralization; with this fix, only local biases remain (Long et al., 2021).

The single CESM simulation is less suited to study the feedback processes between the marine carbon cycle and atmospheric CO_2 as, for example, the effects of the EP on outgassing cannot be easily isolated. To study these feedback processes in more detail, we use the Simple Carbon Project Model v1.0 (SCP-M) (C. M. O'Neill et al., 2019) as described in the Supplementary Information including adaptations from (Boot et al., 2022). The SCP-M consists of seven ocean boxes, one atmosphere box and two terrestrial reservoirs of carbon (Fig. S1) in which many carbon cycle processes are captured in a parameterized way. Processes in the model that affect dissolved inorganic carbon (DIC) and alkalinity (Alk) are the ocean circulation, biological production, calcium carbonate production and dissolution, river fluxes, sediment fluxes and the air-sea gas exchange of CO_2 (DIC only).

3 Results

The prescribed emissions (in Pg CO_2 per year) top in the year 2085 and decrease afterwards (Fig. S2a). By the year 2100, 88 GtC has been emitted into the atmosphere (Meinshausen et al., 2020). Under the influence of the emissions and the exchange with the land and the ocean, the atmospheric CO_2 concentration in the CESM simulation increases from 400 ppm in 2015 to 1069 ppm in 2100 (Fig. S2b). Part of this carbon (Fig. S3a) is taken up by the terrestrial biosphere (6 %), and part by the ocean (6 %). Over time, relatively less carbon is taken up by these two reservoirs, which means more remains in the atmosphere (Fig. S3b).

The changes in the global air-sea gas CO_2 exchange are shown in the upper panels of Fig. 1, where a positive sign indicates CO_2 transfer into the ocean. Whereas almost the entire ocean takes up more (or gasses out less) carbon at the end of the century compared to present-day, the North Atlantic actually takes up less. This becomes even more clear when we compare globally integrated gas exchange with the gas exchange integrated over the North Atlantic. Air-sea gas exchange increases globally until the end of the century but in the North Atlantic, it starts to decrease around the year 2040 (Fig. S4), suggesting substantial carbon cycle changes in the North Atlantic.

The response in the North Atlantic stands out for several reasons. First of all, the warming rate of Sea Surface Temperature (SST) is relatively low in the North Atlantic, and SSTs even decrease locally (Fig. S5). There are also large changes in the annual max-

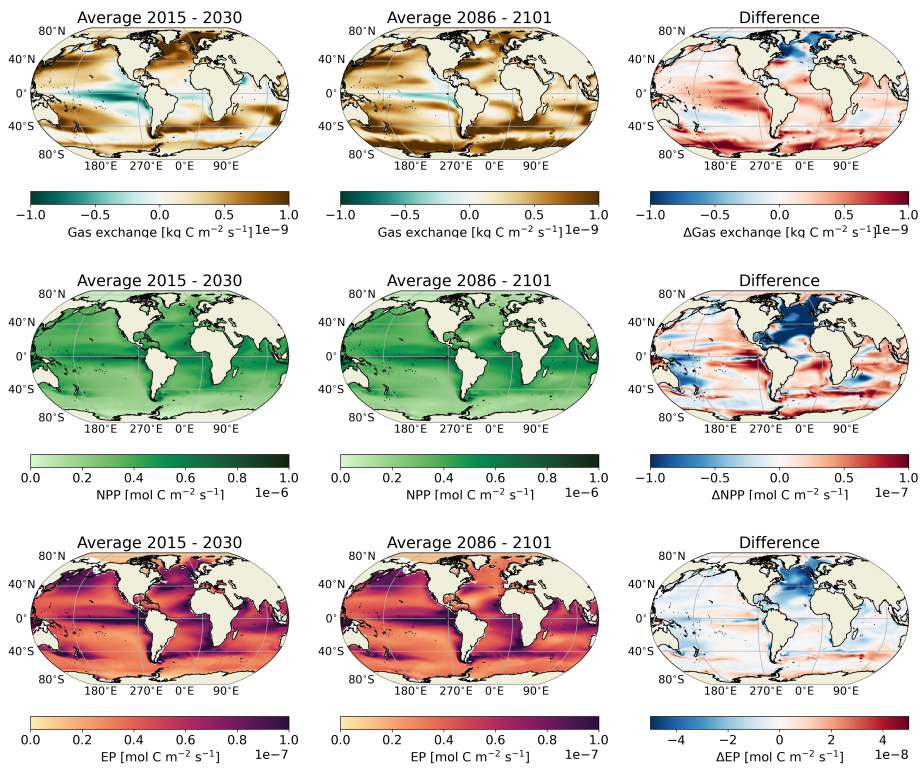

Figure 1. Changes in carbon-cycle relevant quantities in the CESM2 SSP5-8.5 emission driven simulation. Top row: gas exchange in kg C m^{-2} s^{-1}. Middle row: Net Primary Production integrated over top 100m in mol C m^{-2} s^{-1}. Bottom row: Export Production at 100m depth in mol C m^{-2} s^{-1}. Note the different scaling per row; within a row, each subplot is scaled in a similar way. Left column: averages over period 2015-2030; middle column: averaged over period 2086-2101; right column: differences between the two (middle - left).

imum mixed layer depth in the deep water formation regions around Greenland (Fig. S6). These are related to ocean circulation changes in particular a decrease in AMOC strength at 26.5°N from 17 Sv to 10 Sv over the simulation period (Fig. S7). We also see a stronger upper ocean stratification (Fig. S8), where stratification is measured here by the density difference between 200m depth and the surface.

There is a large decrease in both NPP and EP (at 100 m depth) in the North Atlantic region and especially in the deep water formation areas around Greenland (Fig. 1). The decrease in EP cannot completely be explained by a decrease in NPP, since EP decreases more than NPP (Fig. S9). This suggests that the plankton functional types (PFTs) in MARBL respond differently in this region to climate change. Diazotrophs do not play a role here due to temperature limitation and hence we focus on changes in diatoms and small phytoplankton. We can determine the effect of these two PFTs by using the equation (used in CESM2) $NPP_i = \mu_{ref} T_f L_i V_i P_i$. Here i refers to the two PFTs (small phytoplankton and diatoms), μ_{ref} is the maximum C-specific growth rate (which is the same for both PFTs) and T_f is a temperature dependent function. Furthermore, L_i is a light limitation function, V_i a nutrient limitation function, and P_i is the biomass of PFT i. Both diatoms and small phytoplankton are limited by nitrogen (N), phosphorus (P), and iron (Fe); diatoms are also limited by silicate (Si).

In the beginning of the 21st century we see that diatoms are dominant in the high latitude North Atlantic (Fig. 2), whereas small phytoplankton are not very abundant. However, at the end of the century we see a change in PFT dominance as diatoms have almost completely disappeared, while the small phytoplankton NPP and biomass (Fig. S15) have increased. The large decrease in diatom NPP decreases total NPP in this region. This shift in plankton type dominance also explains why the EP decreases faster than the NPP (Fig. S9) since diatoms are more efficient in exporting carbon than small phytoplankton. Since diatoms become less abundant, the carbon transport from the surface to the deep ocean also becomes less efficient.

To investigate why the plankton composition changes in the North Atlantic, and why diatom NPP decreases, we look into what determines the production of the different PFTs. Both PFTs are generally nitrogen limited in this region, though nitrogen limitation is stronger for diatoms. Light limitation decreases by a small amount for the diatoms in the beginning of the 21st century before becoming more or less stable. Light limitation for small phytoplankton decreases throughout the entire century. The difference in light limitation explains mostly the co-limitation: diatom co-limitation of light and nutrients increases, whereas for small phytoplankton it decreases (Figs. S10-S11). We can also see this in the growth rate (NPP divided by biomass) of both PFTs (Fig. S12): the growth rate of diatoms peaks around 2035 and then gradually decreases, and the growth rate of small phytoplankton keeps on increasing.

The reduced growth rate of diatoms does not completely explain the decrease in NPP and biomass, since the biomass of diatoms decreases throughout the entire period (Fig. S13f), while the growth rate of diatoms first increases (Fig. S12). Another reason for the decrease in biomass is advective transport of diatoms out of the North Atlantic (Fig. S13). Looking at the advective fluxes of diatom biomass over the region (45°-70°N $\times$ 270°-0 °E), we can see that in the beginning of the 21st century relatively much biomass is lost due to advection over the southern and eastern boundaries of this region which explains the decreasing NPP over this time period. Total advection decreases mostly due reduced biomass concentrations near the southern boundary (Fig. S13d, e). Small phytoplankton biomass is not affected by this advection, because biomass concentrations are low in the beginning of the boundary of this region century and only increase at the southern boundary of the region when diatom biomass decreases (Fig. S14). Eventually, due to the reduced growth rate, the biomass of diatoms does not recover. This causes the decrease in diatom NPP and explains why small phytoplankton are able to outcompete diatoms in this region utilizing the nutrients not used by diatoms anymore.

The changes in NPP and EP affect the concentrations of DIC and Alk. These two tracers affect the pCO_2 of the surface ocean, and thus the gas exchange with the atmosphere. Within CESM, it is difficult (without further simulations) to determine the effect of the reduced NPP and EP on the air-sea gas exchange and atmospheric pCO_2 as the latter quantity is determined by many other processes which cannot be separated. This effect, however, is crucial for establishing the sign of the plankton composition atmospheric CO_2 feedback associated with changes in EP. To assess the feedback strength, we use the SCP-M model in combination with the CESM2 data.

Compared to the original model (C. M. O'Neill et al., 2019), we updated the SCP-M forcing files for the period 2015-2101 to represent the SSP5-8.5 scenario. We initialize the SCP-M with DIC, Alk and atmospheric CO_2 data from the CESM2 simulation of the year 2015. For the other tracers and the terrestrial biosphere initial conditions are taken from a run performed up until 2014 with historical emissions. The SCP-M captures less dynamics than the CESM2 due to reduced model complexity. We therefore first determine how large this term is to be able to separate this from the feedback strength (Fig. 3e,f). The relative uncaptured processes by the SCP-M amounts up to approximately 8% of the total atmospheric CO_2 concentration of the CESM2. After determining the uncaptured dynamics, we determine the feedback strength by allowing both the DIC and

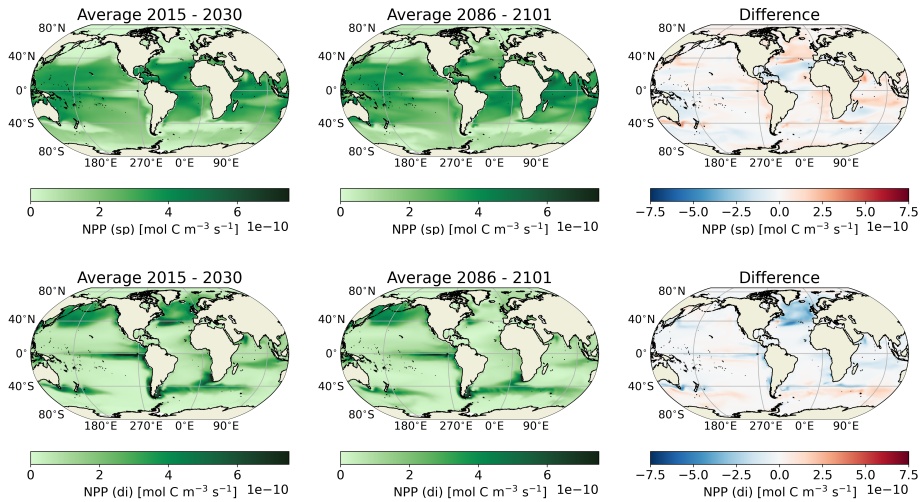

Figure 2. NPP averaged over top 100m in mol C m^{-3} s^{-1} for small phytoplankton (top row) and diatoms (bottom row) for the period 2015-2030 (left), the period 2086-2101 (middle) and the difference between the two (right).

Alk biological fluxes to vary as a function of atmospheric pCO_2 following a fit to CESM2 output (Fig. 3c,d). This fit represents the rate of change of DIC and Alk due to biological activity and the CESM2 output variables are averaged over the region 40°-60°N × 270°-30°E in the top 150m of the water column (Fig. 3a,b).

Using our method we can give a first estimate of the order of magnitude of the feedback. We find that the effect of reduced NPP and EP causes variability in both DIC and Alk which results in a cumulative flux of approximately 294 $GtCO_2$ extra in the atmosphere in the year 2100, resulting in a 37.9 ppm higher CO_2 concentration in the atmosphere (Fig. 4). Over this time period global mean surface temperature rises 4.9 K (average 2096-2100 minus average 2015-2019). This process hence represents a positive feedback with a strength of 60 ($\frac{294}{4.9}$) $GtCO_2$/K warming where, due to increasing CO_2 concentrations, changes in the physical system such as an increase in stratification in the North Atlantic, result in an unfavorable environment for diatoms while small phytoplankton profit. This change in plankton composition decreases the flux of carbon from the surface to the deep ocean which increases DIC and decreases Alk concentrations in the surface ocean. The combined effect results in a decrease in the uptake of CO_2 in the ocean, further increasing atmospheric CO_2 concentrations.

4 Summary and discussion

In this study, we investigated the interaction of atmospheric pCO_2 and biological production in the Atlantic Ocean north of 45°N in an emission driven SSP5-8.5 scenario simulation in CESM2. We found that under these high emissions, net primary production (NPP) and export production (EP) decrease in this region. Similar results on NPP and EP have been obtained in CMIP5 simulations under the RCP8.5 scenario (Bopp et al., 2013). It was shown that in the CESM2 simulation, this could be attributed to reduced productivity of diatoms which could be explained by increasing co-limitation of light and nitrogen and decreasing biomass stocks. The increasing limitation was the result of stronger stratification in the North Atlantic, which could be partly explained by increasing atmospheric temperatures due to increasing atmospheric CO_2 levels. The shift

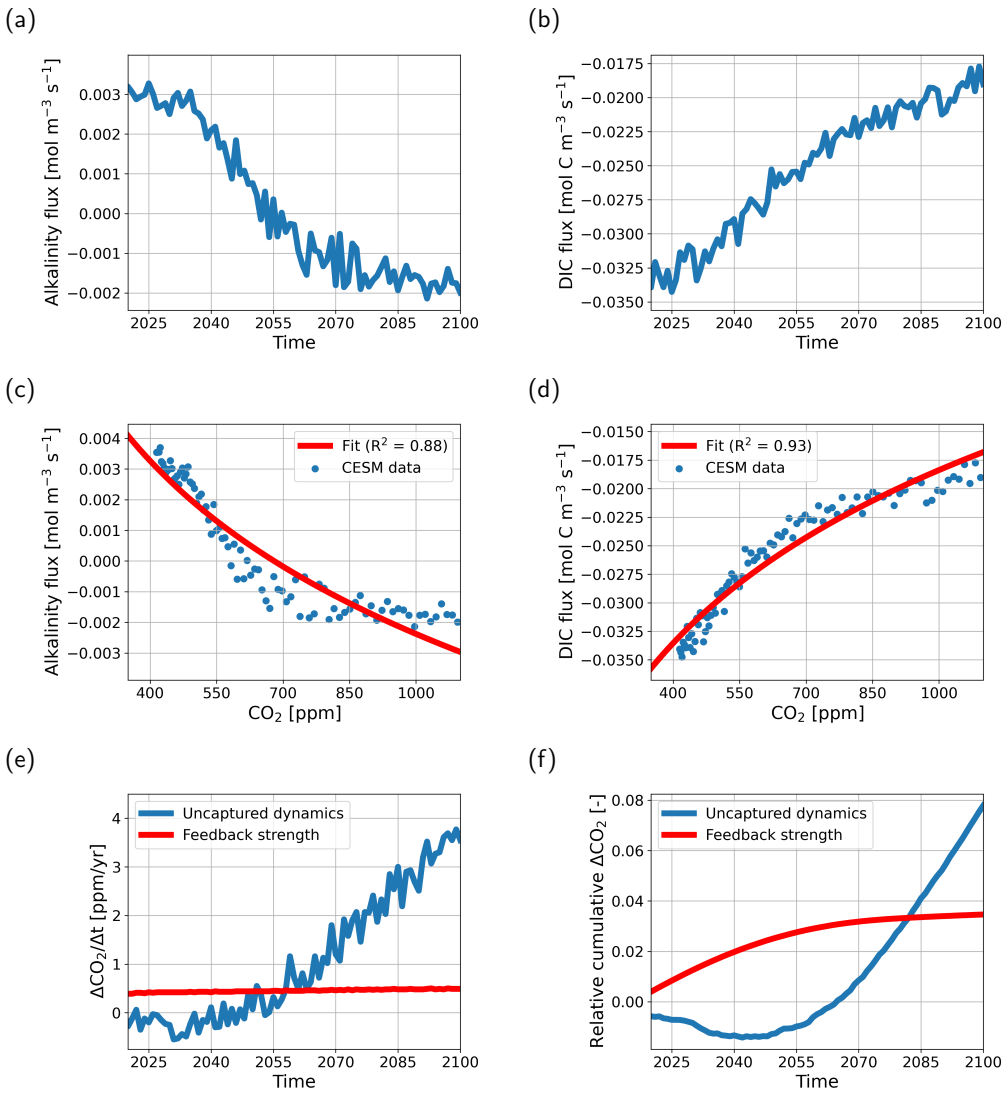

Figure 3. (a) Change of Alk flux in the region 40°-60°N × 270°-30°E in the top 150m of the water column due to biological activity in the CESM2 versus time. (b) As in (a) but for DIC. (c) Blue markers represent CESM2 data as in (a) but versus atmospheric CO_2 concentration, and the red line represents a logarithmic fit to this data. (d) As (c) but for DIC. (e) The uncaptured dynamics for atmospheric CO_2 concentrations in ppm/yr in the SCP-M with respect to CESM2 in blue, and the feedback strength in red. (f) As in (e) but cumulative and relative to the atmospheric CO_2 concentration.

in plankton composition from larger diatoms to small phytoplankton is in agreement with theory and model results suggesting that small phytoplankton outcompete diatoms under increased nutrient stress (Marinov et al., 2013).

The results indicate the existence of a positive carbon cycle feedback where plankton composition plays a central role as shown in Fig. 4. Using an idealized carbon cycle model, we have made a first attempt to put an order of magnitude on the feedback

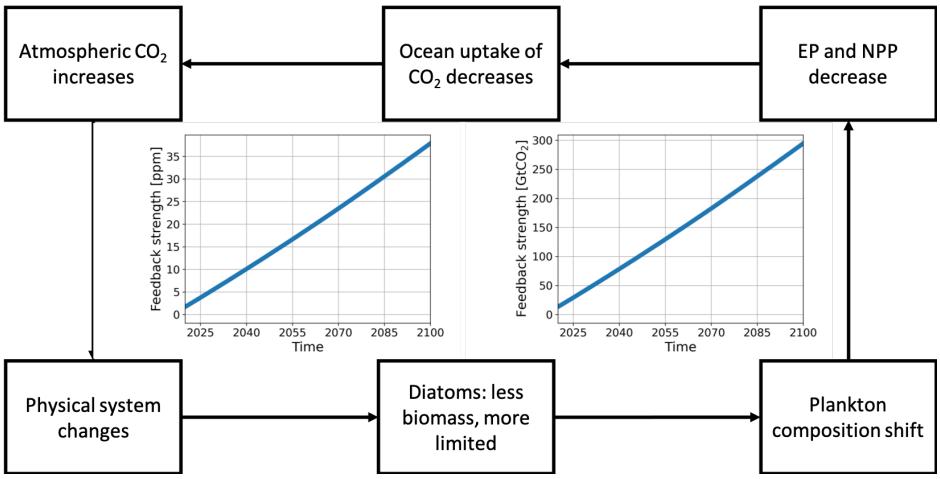

Figure 4. Positive feedback loop on how biological activity in the North Atlantic Ocean is coupled to atmospheric pCO_2. Left graph in the loop represents the increase of atmospheric pCO_2 due to the feedback loop in ppm. The right graph represents the equivalent cumulative change in air-sea gas exchange of CO_2 in $GtCO_2$.

strength. Obviously this method has several caveats since the SCP-M captures less dynamics than the CESM2 and it is therefore difficult to assess the reliability of the results. In our method, the uncaptured dynamics is quite sensitive to initial conditions and parameter values. However, the actual feedback strength is only sensitive to the original strength of the biological flux. Using this simple method, it was shown that this feedback results in an increase in atmospheric CO_2 of 37.9 ppm in 2100, which is equivalent to approximately 294 $GtCO_2$. To put this into perspective, this is slightly smaller than the increased CO_2 storage of $\sim$ 336 $GtCO_2$ in the North Atlantic in the Last Glacial Maximum due to a more efficient biological carbon pump (Yu et al., 2019), meaning that the order of magnitude of our feedback strength is in a realistic range. This positive feedback (Cabré et al., 2015) seems to be relatively small, but it needs to be taken into account when estimating the safe carbon budget in future climate change. The safe carbon budget is estimated to be 308 $GtCO_2$ for a peak global warming of 1.5 K, and 994 $GtCO_2$ for a warming of 2 K (van der Ploeg, 2018). Assuming the assessed feedback strength is correct, this feedback accounts for approximately 29% and 12% of the 1.5 K and 2.0 K warming safe carbon budget respectively. In summary, biological activity in the ocean is able to interact with the physical system and have an impact on variables such as global mean surface temperature via atmospheric CO_2 concentrations, with a substantial impact on our safe carbon budget. Furthermore, we want to stress that the numbers presented here should be viewed as an estimate on the order of magnitude of the feedback strength and not as an exact result because the used method to asses the feedback strength has multiple caveats.

Certainly this study has its limitations, as only a single Earth System Model with only a single member simulation for only one emission scenario is used. It might be very interesting to repeat such simulations and analysis with models having different plankton dynamics since responses of Earth System Models depend on the complexity of this dynamics (Dutkiewicz et al., 2013; Fu et al., 2016) and since there exists a large intermodel spread in NPP and EP among CMIP6 models (Kwiatkowski et al., 2020; Tagliabue et al., 2021). Furthermore, it would be useful to extend such simulations to, for example, 2300 to see whether the increased productivity of the small phytoplankton groups

are able to dampen the positive feedback, or whether they will also become more limited due to increasing stratification in the North Atlantic.

Appendix A Open Research

The Community Earth System Model v2 (CESM2) output can be downloaded from the Earth System Grid Federation (ESGF) (`https://esgf-node.llnl.gov/search/cmip6/`) (Danabasoglu, 2019). Processed datasets, scripts for plotting, and scripts related to the Simple Carbon Project Model (SCP-M) used for this study can be found at `10.5281/zenodo.6770132` (Boot et al., 2022). We have also included a list of datasets downloaded from the ESGF which are necessary to create the processed datasets, and the figures. The original SCP-M V1.0 can be found at `10.5281/zenodo.1310161` (C. M. O'Neill et al., 2018).

Acknowledgments

This study has been supported by the Netherlands Earth System Science Centre (NESSC), which is financially supported by the Ministry of Education, Culture and Science (OCW; grant no. 024.002.001)

References

Archer, D., & Maier-Reimer, E. (1994). Effect of deep-sea sedimentary calcite preservation on atmospheric CO2 concentration. *Nature*, *367*(6460), 260–263. Retrieved from `https://doi.org/10.1038/367260a0` doi: 10.1038/367260a0

Beaugrand, G. (2009). Decadal changes in climate and ecosystems in the North Atlantic Ocean and adjacent seas. *Deep Sea Research Part II: Topical Studies in Oceanography*, *56*(8), 656–673. Retrieved from `https://www.sciencedirect.com/science/article/pii/S0967064508004244` doi: https://doi.org/10.1016/j.dsr2.2008.12.022

Behrenfeld, M. J., O'Malley, R. T., Siegel, D. A., McClain, C. R., Sarmiento, J. L., Feldman, G. C., … Boss, E. S. (2006). Climate-driven trends in contemporary ocean productivity. *Nature*, *444*(7120), 752–755. Retrieved from `https://doi.org/10.1038/nature05317` doi: 10.1038/nature05317

Bennington, V., McKinley, G. A., Dutkiewicz, S., & Ullman, D. (2009). What does chlorophyll variability tell us about export and air-sea CO2 flux variability in the North Atlantic? *Global Biogeochemical Cycles*, *23*(3). Retrieved from `https://doi.org/10.1029/2008GB003241` doi: https://doi.org/10.1029/2008GB003241

Boot, A., von der Heydt, A. S., & Dijkstra, H. A. (2022, June). *Plankton composition shift CESM2.* [dataset]. Zenodo. doi: 10.5281/zenodo.6770132

Bopp, L., Aumont, O., Cadule, P., Alvain, S., & Gehlen, M. (2005). Response of diatoms distribution to global warming and potential implications: A global model study. *Geophysical Research Letters*, *32*(19). Retrieved from `https://doi.org/10.1029/2005GL023653` doi: https://doi.org/10.1029/2005GL023653

Bopp, L., Monfray, P., Aumont, O., Dufresne, J.-L., Le Treut, H., Madec, G., … Orr, J. C. (2001). Potential impact of climate change on marine export production. *Global Biogeochemical Cycles*, *15*(1), 81–99. Retrieved from `https://doi.org/10.1029/1999GB001256` doi: https://doi.org/10.1029/1999GB001256

Bopp, L., Resplandy, L., Orr, J. C., Doney, S. C., Dunne, J. P., Gehlen, M., … Vichi, M. (2013, oct). Multiple stressors of ocean ecosystems in the 21st century: projections with CMIP5 models. *Biogeosciences*, *10*(10),

6225–6245. Retrieved from https://bg.copernicus.org/articles/10/6225/2013/https://bg.copernicus.org/articles/10/6225/2013/bg-10-6225-2013.pdf doi: 10.5194/bg-10-6225-2013

Cabré, A., Marinov, I., & Leung, S. (2015). Consistent global responses of marine ecosystems to future climate change across the IPCC AR5 earth system models. *Climate Dynamics*, *45*(5), 1253–1280. Retrieved from https://doi.org/10.1007/s00382-014-2374-3 doi: 10.1007/s00382-014-2374-3

Danabasoglu, G. (2019). *Ncar cesm2 model output prepared for cmip6 c4mip esm-ssp585.* Earth System Grid Federation. Retrieved from https://doi.org/10.22033/ESGF/CMIP6.7582 doi: 10.22033/ESGF/CMIP6.7582

Danabasoglu, G., Lamarque, J.-F., Bacmeister, J., Bailey, D. A., DuVivier, A. K., Edwards, J., ... Strand, W. G. (2020). The Community Earth System Model Version 2 (CESM2). *Journal of Advances in Modeling Earth Systems*, *12*(2), e2019MS001916. Retrieved from https://doi.org/10.1029/2019MS001916 doi: https://doi.org/10.1029/2019MS001916

DeVries, T., Holzer, M., & Primeau, F. (2017). Recent increase in oceanic carbon uptake driven by weaker upper-ocean overturning. *Nature*, *542*(7640), 215–218. Retrieved from https://doi.org/10.1038/nature21068 doi: 10.1038/nature21068

Doney, S. C., Ruckelshaus, M., Emmett Duffy, J., Barry, J. P., Chan, F., English, C. A., ... Talley, L. D. (2011, dec). Climate Change Impacts on Marine Ecosystems. *Annual Review of Marine Science*, *4*(1), 11–37. Retrieved from https://doi.org/10.1146/annurev-marine-041911-111611 doi: 10.1146/annurev-marine-041911-111611

Dutkiewicz, S., Scott, J. R., & Follows, M. J. (2013). Winners and losers: Ecological and biogeochemical changes in a warming ocean. *Global Biogeochemical Cycles*, *27*(2), 463–477. Retrieved from https://doi.org/10.1002/gbc.20042 doi: https://doi.org/10.1002/gbc.20042

Eyring, V., Bony, S., Meehl, G. A., Senior, C. A., Stevens, B., Stouffer, R. J., & Taylor, K. E. (2016, may). Overview of the Coupled Model Intercomparison Project Phase 6 (CMIP6) experimental design and organization. *Geosci. Model Dev.*, *9*(5), 1937–1958. Retrieved from https://gmd.copernicus.org/articles/9/1937/2016/https://gmd.copernicus.org/articles/9/1937/2016/gmd-9-1937-2016.pdf doi: 10.5194/gmd-9-1937-2016

Fu, W., Randerson, J. T., & Moore, J. K. (2016, sep). Climate change impacts on net primary production (NPP) and export production (EP) regulated by increasing stratification and phytoplankton community structure in the CMIP5 models. *Biogeosciences*, *13*(18), 5151–5170. Retrieved from https://bg.copernicus.org/articles/13/5151/2016/https://bg.copernicus.org/articles/13/5151/2016/bg-13-5151-2016.pdf doi: 10.5194/bg-13-5151-2016

Green, C., Carlisle, D., O'Neill, B. C., van Ruijven, B. J., Boyer, C., & Ebi, K. (2021). *Shared socioeconomic pathways (ssps) literature database, v1, 2014-2019.* NASA Socioeconomic Data and Applications Center (SEDAC). Retrieved from https://doi.org/10.7927/hn96-9703 doi: 10.7927/hn96-9703

Henson, S. A., Laufkötter, C., Leung, S., Giering, S. L. C., Palevsky, H. I., & Cavan, E. L. (2022). Uncertain response of ocean biological carbon export in a changing world. *Nature Geoscience*, *15*(4). Retrieved from https://doi.org/10.1038/s41561-022-00927-0 doi: 10.1038/s41561-022-00927-0

Hilligsøe, K. M., Richardson, K., Bendtsen, J., Sørensen, L.-L., Nielsen, T. G., & Lyngsgaard, M. M. (2011). Linking phytoplankton community size composition with temperature, plankton food web structure and sea–air CO2 flux. *Deep Sea Research Part I: Oceanographic Research Papers*, *58*(8), 826–838. Retrieved from https://www.sciencedirect.com/science/article/pii/S0967063711001142 doi: https://doi.org/10.1016/j.dsr.2011.06.004

Ito, T., & Follows, M. J. (2005). Preformed phosphate, soft tissue pump and atmospheric CO2. *Journal of Marine Research*, *63*(4), 813–839. Retrieved from https://www.ingentaconnect.com/content/jmr/jmr/2005/00000063/00000004/art00007 doi: doi:10.1357/0022240054663231

Kohfeld, K. E., Le, Q. C., P., H. S., & F., A. R. (2005, apr). Role of Marine Biology in Glacial-Interglacial CO2 Cycles. *Science*, *308*(5718), 74–78. Retrieved from https://doi.org/10.1126/science.1105375 doi: 10.1126/science.1105375

Kwiatkowski, L., Torres, O., Bopp, L., Aumont, O., Chamberlain, M., Christian, J. R., ... Ziehn, T. (2020). Twenty-first century ocean warming, acidification, deoxygenation, and upper-ocean nutrient and primary production decline from cmip6 model projections. *Biogeosciences*, *17*(13), 3439–3470. Retrieved from https://bg.copernicus.org/articles/17/3439/2020/ doi: 10.5194/bg-17-3439-2020

Lenton, T. M., Rockström, J., Gaffney, O., Rahmstorf, S., Richardson, K., Steffen, W., & Schellnhuber, J. (2019). Climate tipping points - too risky to bet against. *Nature*, *575*, 592–595. doi: 10.1038/d41586-019-03595-0

Li, W. K. W., McLaughlin, F. A., Lovejoy, C., & Carmack, E. C. (2009, oct). Smallest Algae Thrive As the Arctic Ocean Freshens. *Science*, *326*(5952), 539. Retrieved from https://doi.org/10.1126/science.1179798 doi: 10.1126/science.1179798

Long, M. C., Moore, J. K., Lindsay, K., Levy, M., Doney, S. C., Luo, J. Y., ... Sylvester, Z. T. (2021). Simulations With the Marine Biogeochemistry Library (MARBL). *Journal of Advances in Modeling Earth Systems*, *13*(12), e2021MS002647. Retrieved from https://doi.org/10.1029/2021MS002647 doi: https://doi.org/10.1029/2021MS002647

Marinov, I., Doney, S. C., Lima, I. D., Lindsay, K., Moore, J. K., & Mahowald, N. (2013). North-South asymmetry in the modeled phytoplankton community response to climate change over the 21st century. *Global Biogeochemical Cycles*, *27*(4), 1274–1290. Retrieved from https://doi.org/10.1002/2013GB004599 doi: https://doi.org/10.1002/2013GB004599

Martinez, E., Antoine, D., D'Ortenzio, F., & de Boyer Montégut, C. (2011). Phytoplankton spring and fall blooms in the North Atlantic in the 1980s and 2000s. *Journal of Geophysical Research: Oceans*, *116*(C11). Retrieved from https://doi.org/10.1029/2010JC006836 doi: https://doi.org/10.1029/2010JC006836

Matthews, D. H., Tokarska, K. B., Rogelj, J., Smith, C. J., MacDougall, A. H., Haustein, K., ... Knutti, R. (2021). An integrated approach to quantifying uncertainties in the remaining carbon budget. *Communications Earth & Environment*, *2*(1), 7. Retrieved from https://doi.org/10.1038/s43247-020-00064-9 doi: 10.1038/s43247-020-00064-9

Meinshausen, M., Nicholls, Z. R. J., Lewis, J., Gidden, M. J., Vogel, E., Freund, M., ... Wang, R. H. J. (2020, aug). The shared socio-economic pathway (SSP) greenhouse gas concentrations and their extensions to 2500. *Geosci. Model Dev.*, *13*(8), 3571–3605. Retrieved from https://gmd.copernicus.org/articles/13/3571/2020/https://gmd.copernicus.org/articles/13/3571/2020/gmd-13-3571-2020.pdf doi: 10.5194/gmd-13-3571-2020

Moore, C. M., Mills, M. M., Arrigo, K. R., Berman-Frank, I., Bopp, L., Boyd, P. W., ... Ulloa, O. (2013). Processes and patterns of oceanic nutrient limitation. *Nature Geoscience*, *6*(9), 701–710. Retrieved from https://doi.org/10.1038/ngeo1765 doi: 10.1038/ngeo1765

Moore, J. K., Fu, W., Primeau, F., Britten, G. L., Lindsay, K., Long, M., ... Randerson, J. T. (2018, mar). Sustained climate warming drives declining marine biological productivity. *Science*, *359*(6380), 1139 LP – 1143. Retrieved from http://science.sciencemag.org/content/359/6380/1139.abstract doi: 10.1126/science.aao6379

Morán, X. A. G., LÓPEZ-URRUTIA, Á., CALVO-DÍAZ, A., & LI, W. K. W. (2010). Increasing importance of small phytoplankton in a warmer ocean. *Global Change Biology*, *16*(3), 1137–1144. Retrieved from https://doi.org/10.1111/j.1365-2486.2009.01960.x doi: https://doi.org/10.1111/j.1365-2486.2009.01960.x

O'Neill, B. C., Carter, T. R., Ebi, K., Harrison, P. A., Kemp-Benedict, E., Kok, K., ... Green, C. (2020). Achievements and needs for the climate change scenario framework. *Nature Climate Change*, *10*. Retrieved from https://doi.org/10.1038/s41558-020-00952-0 doi: 10.1038/s41558-020-00952-0

O'Neill, C. M., Hogg, A. M., Ellwood, M. J., Eggins, S. M., & Opdyke, B. N. (2019). The [simple carbon project] model v1.0. *Geoscientific Model Development*, *12*(4), 1541–1572. Retrieved from https://gmd.copernicus.org/articles/12/1541/2019/ doi: 10.5194/gmd-12-1541-2019

O'Neill, C. M., Hogg, A. M., Ellwood, M. J., Opdyke, B. N., & Eggins, S. M. (2018). *[simple carbon project] model (v1.0).* [code]. Zenodo. Retrieved from https://doi.org/10.5281/zenodo.1310161 doi: 10.5281/zenodo.1310161

Osman, M. B., Das, S. B., Trusel, L. D., Evans, M. J., Fischer, H., Grieman, M. M., ... Saltzman, E. S. (2019). Industrial-era decline in subarctic Atlantic productivity. *Nature*, *569*(7757), 551–555. Retrieved from https://doi.org/10.1038/s41586-019-1181-8 doi: 10.1038/s41586-019-1181-8

Richardson, A. J., & Schoeman, D. S. (2004, sep). Climate impact on plankton ecosystems in the Northeast Atlantic. *Science (New York, N.Y.)*, *305*(5690), 1609–1612. doi: 10.1126/science.1100958

Rivero-Calle, S., Gnanadesikan, A., Del Castillo, E. C., M., B. W., & D., G. S. (2015, dec). Multidecadal increase in North Atlantic coccolithophores and the potential role of rising CO2. *Science*, *350*(6267), 1533–1537. Retrieved from https://doi.org/10.1126/science.aaa8026 doi: 10.1126/science.aaa8026

Sabine, C. L., Feely, R. A., Gruber, N., Key, R. M., Lee, K., Bullister, J. L., ... Rios, A. F. (2004, jul). The oceanic sink for anthropogenic CO2. *Science (New York, N.Y.)*, *305*(5682), 367–371. doi: 10.1126/science.1097403

Sanders, R., Henson, S. A., Koski, M., De La Rocha, C. L., Painter, S. C., Poulton, A. J., ... Martin, A. P. (2014). The Biological Carbon Pump in the North Atlantic. *Progress in Oceanography*, *129*, 200–218. Retrieved from https://www.sciencedirect.com/science/article/pii/S0079661114000901 doi: https://doi.org/10.1016/j.pocean.2014.05.005

Schmittner, A. (2005). Decline of the marine ecosystem caused by a reduction in the Atlantic overturning circulation. *Nature*, *434*(7033), 628–633. Retrieved from https://doi.org/10.1038/nature03476 doi: 10.1038/nature03476

Séférian, R., Berthet, S., Yool, A., Palmiéri, J., Bopp, L., Tagliabue, A., ... Yamamoto, A. (2020). Tracking Improvement in Simulated Marine Biogeochemistry Between CMIP5 and CMIP6. *Current Climate Change Reports*, *6*(3), 95–119. Retrieved from https://doi.org/10.1007/s40641-020-00160-0 doi: 10.1007/s40641-020-00160-0

Smith, R., Jones, P. W., Briegleb, P. A., Bryan, O., Danabasoglu, G., Dennis, M. L., ... Yeager, S. G. (2010). The Parallel Ocean Program (POP) reference manual: Ocean component of the Community Climate System Model (CCSM)..

Steinacher, M., Joos, F., Frölicher, T. L., Bopp, L., Cadule, P., Cocco, V., ... Segschneider, J. (2010, mar). Projected 21st century decrease in marine productivity: a multi-model analysis. *Biogeosciences*, *7*(3), 979–1005. Retrieved from https://bg.copernicus.org/articles/7/979/2010/https://bg.copernicus.org/articles/7/979/2010/bg-7-979-2010.pdf doi: 10.5194/bg-7-979-2010

Tagliabue, A., Kwiatkowski, L., Bopp, L., Butenschön, M., Cheung, W., Lengaigne, M., & Vialard, J. (2021). Persistent uncertainties in ocean net primary

production climate change projections at regional scales raise challenges for assessing impacts on ecosystem services. *Frontiers in Climate*, *3*. Retrieved from https://www.frontiersin.org/article/10.3389/fclim.2021.738224 doi: 10.3389/fclim.2021.738224

van der Ploeg, F. (2018). The safe carbon budget. *Climatic Change*, *147*(1), 47–59. Retrieved from https://doi.org/10.1007/s10584-017-2132-8 doi: 10.1007/s10584-017-2132-8

Yu, J., Menviel, L., Jin, Z. D., Thornalley, D. J. R., Foster, G. L., Rohling, E. J., ... Roberst, A. P. (2019). More efficient north atlantic carbon pump during the last glacial maximum. *Nature Communications*, *10*(1). Retrieved from https://doi.org/10.1038/s41467-019-10028-z doi: 10.1038/s41467-019-10028-z

Supporting Information for "Effect of plankton composition shifts in the North Atlantic on atmospheric pCO_2"

A. Boot[1], A. S. von der Heydt[1,2], and H. A. Dijkstra[1,2]

[1]Institute for Marine and Atmospheric research Utrecht, Department of Physics,Utrecht University, Utrecht, the Netherlands

[2]Center for Complex Systems Studies, Utrecht University, Utrecht, the Netherlands

Contents of this file

1. The Simple Carbon Project Model v1.0
2. Figures S1 to S14

Introduction The supporting information contains a more elaborate explanation of the Simple Carbon Project Model v1.0 (SCP-M). Furthermore, it contains a figure of the model structure of the SCP-M and more results of the CESM2.

The Simple Carbon Project Model v1.0 In this study, we have used the Simple Carbon Project Model v1.0 (SCP-M) and the model description is based on earlier work (Boot et al., 2022). For a complete description we refer the reader to the original paper (C. M. O'Neill et al., 2019). The SCP-M is a carbon cycle box model with a focus on the carbon cycle in the ocean. Several tracers are resolved in the ocean among which

dissolved inorganic carbon and alkalinity. In the ocean, circulation, air-sea gas exchange, biological production, calcium carbonate production and dissolution, river fluxes and sediment fluxes are resolved but mostly in a very parameterized way. Besides an oceanic part, there are also two terrestrial biosphere carbon stocks and anthropogenic emissions to the atmosphere.

The model consists of 10 boxes: 1 atmosphere box, 7 ocean boxes, and 2 boxes in the terrestrial biosphere (Fig. S1). There is no explicit sediment box in this model. This is a 2D box model with dimensions in the vertical and latitudinal direction, meaning that there is no dependence on longitude or ocean basins. Box 2 represents the northern high latitude box and therefore the North Atlantic.

Carbon and alkalinity in Box 2 are affected by the Atlantic Meridional Overturning Circulation (AMOC, ψ_2, orange arrow in Fig. S1), biological production (green arrow in Fig. S1), calcium carbonate production and dissolution (light gray arrow and wiggle in Fig. S1), and air-sea gas exchange (carbon only; dark gray arrow in Fig. S1). From these processes the AMOC, the biological and calcium carbonate production are constant in the model. Calcium carbonate dissolution is saturation dependent and therefore dependent on the pH of the ocean water. This pH is determined using a direct solver which uses the pH from the previous time step as a first estimate (Follows et al., 2006). To increase accuracy we run the solver twice each time step (note that in the original model the solver is run once). With the pH, oceanic pCO_2 can also be determined which is important for the air-sea gas exchange of CO_2, which is also dependent on the CO_2 concentration in the

atmosphere. Temperature is affected by anthropogenic forcing, but this is prescribed and not dependent on atmospheric pCO_2; the salinity is constant.

For the purpose of studying the feedback processes we have made slight adaptations to the SCP-M. First of all, we have included biological fluxes that affect alkalinity following

$$A_{bio} = -\frac{16}{106} C_{bio} \tag{1}$$

Where A_{bio} is the biological alkalinity flux, C_{bio} the biological carbon flux, and the fraction $\frac{16}{106}$ represents the uptake of nitrate following constant stoichiometric ratios. Just as the biological DIC flux, it is constant. Secondly, we have updated the anthropogenic forcing to represent SSP5-8.5 instead of RCP8.5 (B. C. O'Neill et al., 2020; Green et al., 2021). And lastly, we have included the option for variable biological fluxes in the North Atlantic as a function of atmospheric pCO_2. This function is determined from fitting CESM2 biological fluxes to CESM2 atmospheric pCO_2 (Fig. 3c,d in the main text) and scaled to the original, constant fluxes in the SCP-M:

$$C_{bio,2} = \frac{pCO_2 * 0.0165 - 0.133}{pCO_{2,0} * 0.0165 - 0.133} \times -2.87 \times 10^{-10} \tag{2}$$

$$A_{bio,2} = \frac{-pCO_2 * 0.00616 + 0.0402}{|-pCO_{2,0} * 0.00616 + 0.0402|} \times \frac{16}{106} \times 2.87 \times 10^{-10} \tag{3}$$

To determine the feedback strength we choose initial conditions in the SCP-M for the year 2015 from CESM2 output for DIC and Alk averaged over the regions corresponding to the boxes. First, we determine the uncaptured dynamics in the SCP-M with respect to the CESM2 with regard to atmospheric pCO_2 for every time step. For this we use constant biological fluxes for all boxes in the SCP-M. Initial conditions for each timestep

are adapted with a uncaptured dynamics parameter Y(t), following

$$pCO_2^{SCPM*}(t) = pCO_2^{SCPM}(t) + Y(t) \tag{4}$$

Where we determine Y(t) using a secant method, such that

$$pCO_2^{SCPM}(t+1) = pCO_2^{CESM}(t+1) \tag{5}$$

After determining the uncaptured dynamics, we can determine the feedback strength. To do this, we use the variable biological fluxes in the North Atlantic box as a function of atmospheric pCO_2 (Eq. 2 and 3). We then determine the feedback strength X(t) for each time step following a similar method:

$$pCO_2^{SCPM*}(t) = pCO_2^{SCPM}(t) + Y(t) + X(t) \tag{6}$$

Where we search for X(t), again using a secant method, such that

$$pCO_2^{SCPM}(t+1) = pCO_2^{CESM2}(t+1) \tag{7}$$

Note that if X(t) is negative, the feedback strength is positive, i.e. we have to lower our 'initial' atmospheric CO_2 concentration, because the ocean takes up less carbon causing more atmospheric pCO_2 to reside in the atmosphere.

References

Boot, A., von der Heydt, A. S., & Dijkstra, H. A. (2022, jul). Effect of the Atlantic Meridional Overturning Circulation on Atmospheric pCO2 Variations. *Earth Syst. Dynam. (in press)*, 1–26. Retrieved from `https://esd.copernicus.org/preprints/esd-2021-42/https://esd.copernicus.org/preprints/esd-2021-42/esd-2021-42.pdf` doi: 10.5194/esd-2021-42

Follows, M. J., Ito, T., & Dutkiewicz, S. (2006). On the solution of the carbonate chemistry system in ocean biogeochemistry models. *Ocean Modelling*, *12*(3), 290–301. Retrieved from http://www.sciencedirect.com/science/article/pii/S1463500305000533 doi: https://doi.org/10.1016/j.ocemod.2005.05.004

Green, C., Carlisle, D., O'Neill, B. C., van Ruijven, B. J., Boyer, C., & Ebi, K. (2021). *Shared socioeconomic pathways (ssps) literature database, v1, 2014-2019.* NASA Socioeconomic Data and Applications Center (SEDAC). Retrieved from https://doi.org/10.7927/hn96-9703 doi: 10.7927/hn96-9703

O'Neill, B. C., Carter, T. R., Ebi, K., Harrison, P. A., Kemp-Benedict, E., Kok, K., ... Green, C. (2020). Achievements and needs for the climate change scenario framework. *Nature Climate Change*, *10*. Retrieved from https://doi.org/10.1038/s41558-020-00952-0 doi: 10.1038/s41558-020-00952-0

O'Neill, C. M., Hogg, A. M., Ellwood, M. J., Eggins, S. M., & Opdyke, B. N. (2019). The [simple carbon project] model v1.0. *Geoscientific Model Development*, *12*(4), 1541–1572. Retrieved from https://gmd.copernicus.org/articles/12/1541/2019/ doi: 10.5194/gmd-12-1541-2019

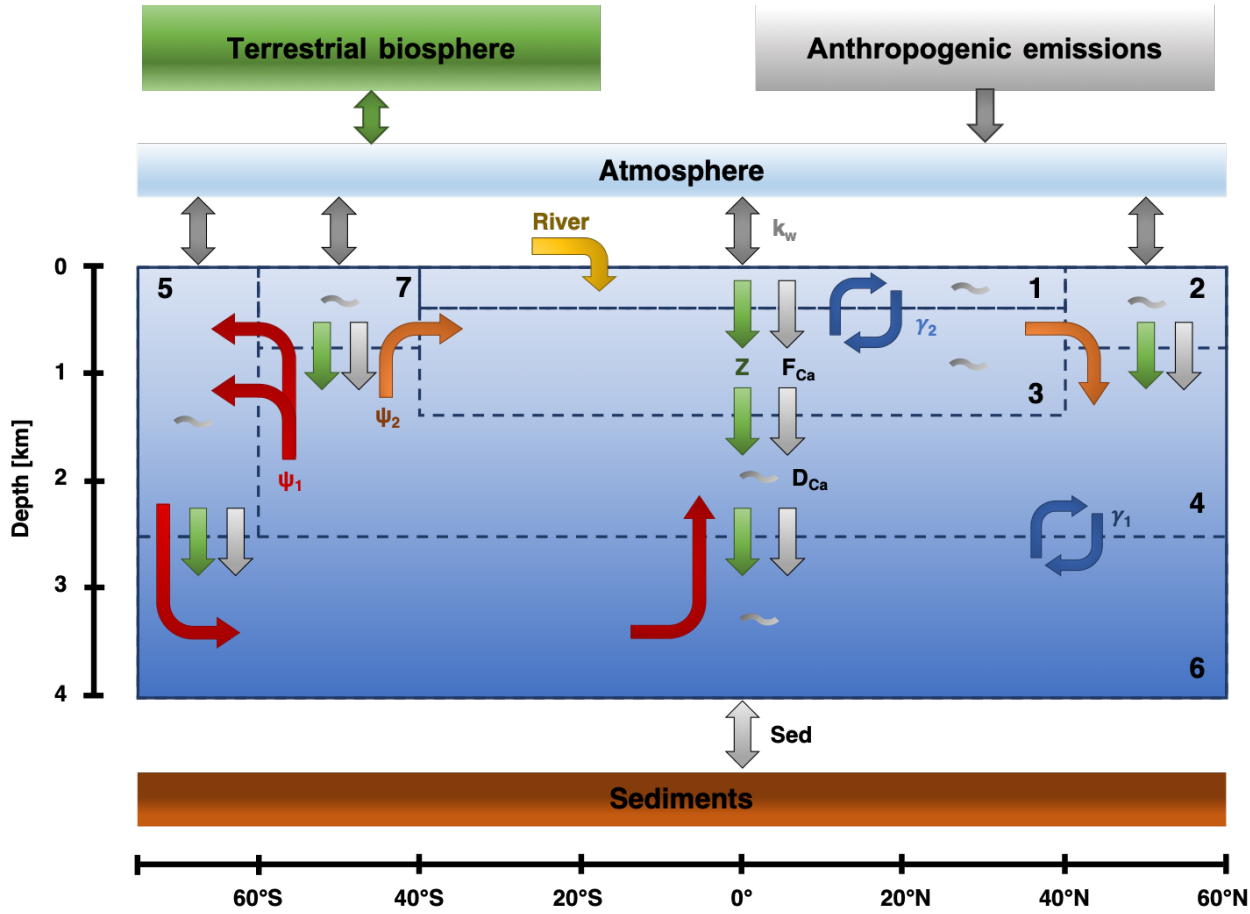

Figure S1. Box structure of the SCP-M. Box 2 represents the northern high latitude ocean. Figure adapted from (Boot et al., 2022).

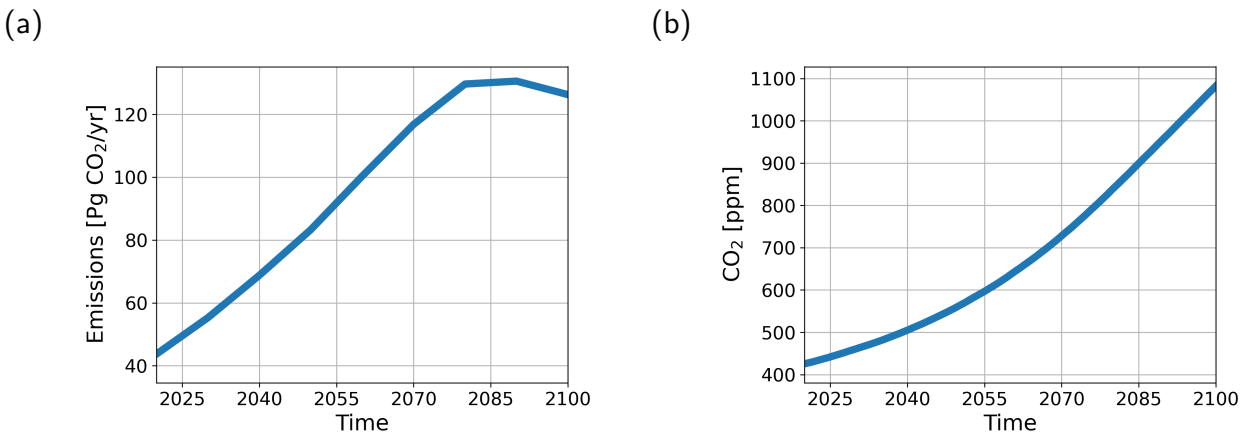

Figure S2. (a) Emissions of CO_2 in Pg CO_2 per year in the SSP5-8.5 scenario. (b) CO_2 concentrations in ppm as simulated in CESM2.

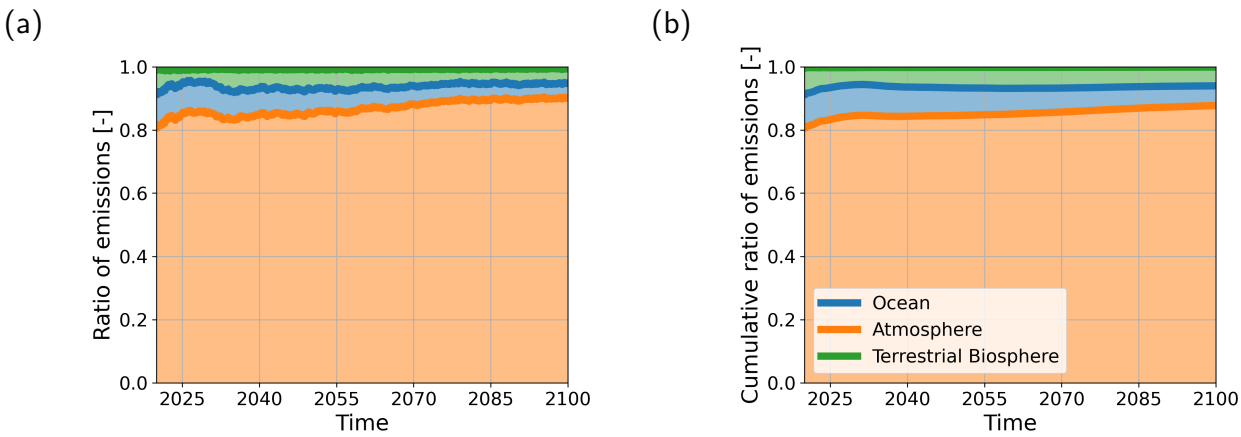

Figure S3. (a) Ratio of how the emitted CO_2 is distributed over the three different reservoirs atmosphere (orange), ocean (blue) and terrestrial biosphere (green) per time step in CESM2. (b) As in (a) but cumulative.

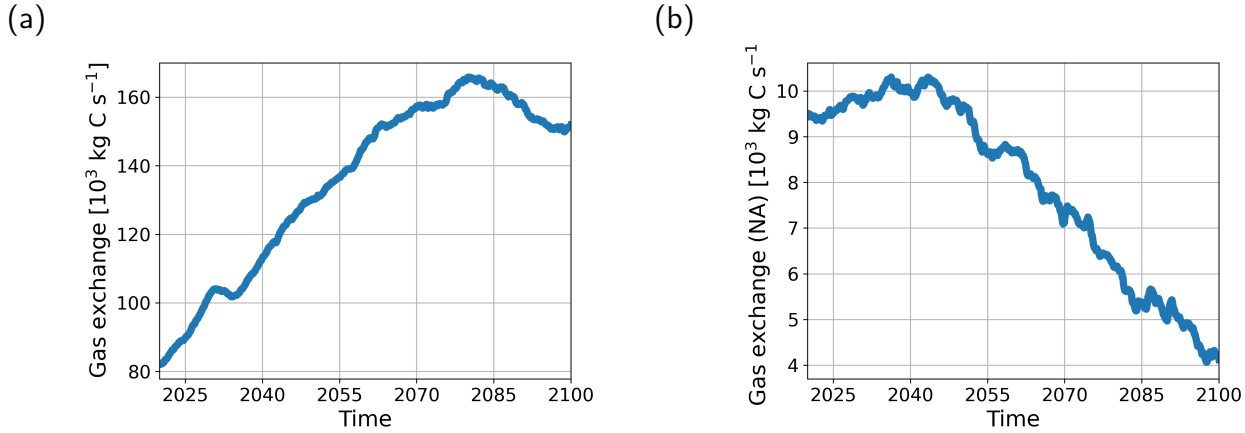

Figure S4. (a) Globally integrated air-sea gas exchange in 10^{-3} kg C s^{-1} in CESM2. (b) As in a, but integrated over the high latitude North Atlantic (45°-70°N × 270°-30°E).

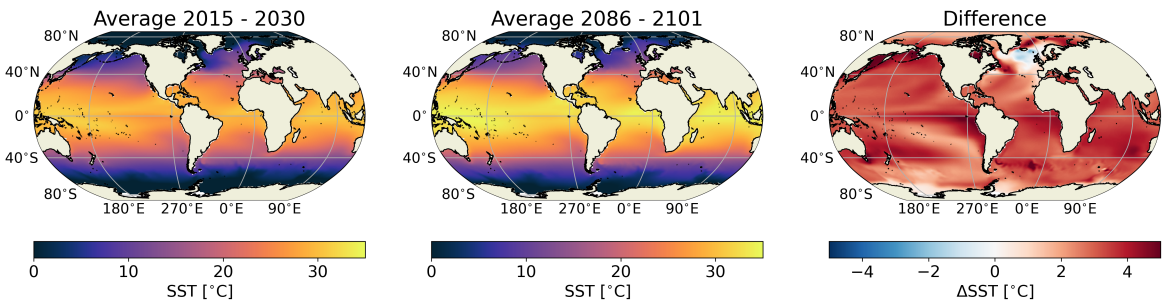

Figure S5. (a) Sea surface temperatures averaged over 2015-2030 in ° C in CESM2. (b) As in (a) but for the period 2086-2101. (c) The difference between the two. Red colors represent warming over the century, blue colors cooling.

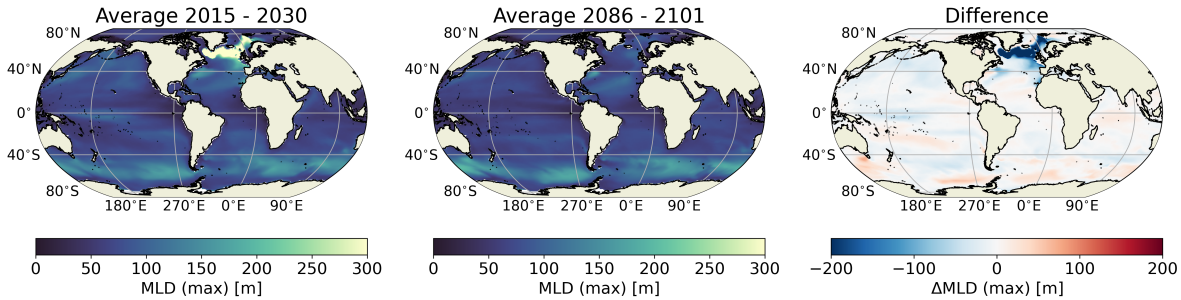

Figure S6. (a) Annual maximum mixed layer depth in m averaged over 2015-2030 in CESM2. (b) As in (a) but for the period 2086-2101. (c) The difference between the two. Red colors represent increasing depth over the century, blue colors decreasing depth.

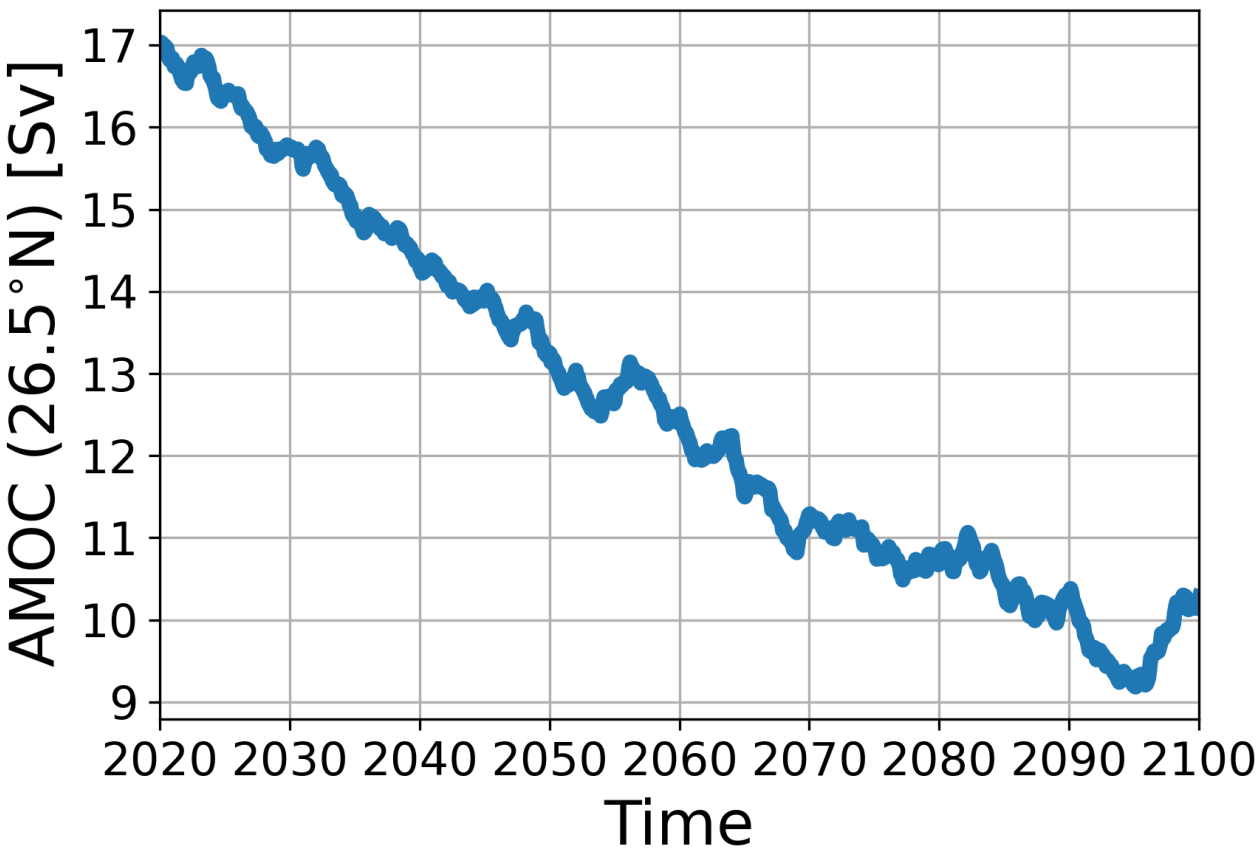

Figure S7. AMOC strength at 26.5°N in Sv as simulated in CESM2.

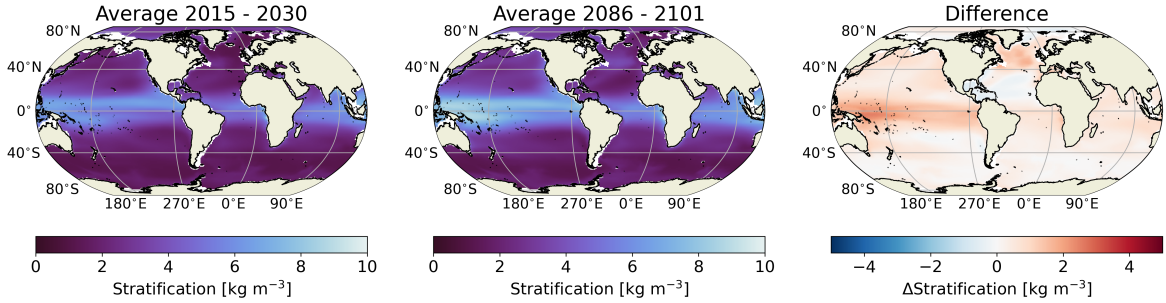

Figure S8. (a) Stratification in kg m^{-3} averaged over 2015-2030 in CESM2. Stratification is measured as the density difference between the surface and z=200 m. (b) As in (a) but for the period 2086-2101. (c) The difference between the two. Red colors represent increasing stratification over the century, blue colors decreasing stratification.

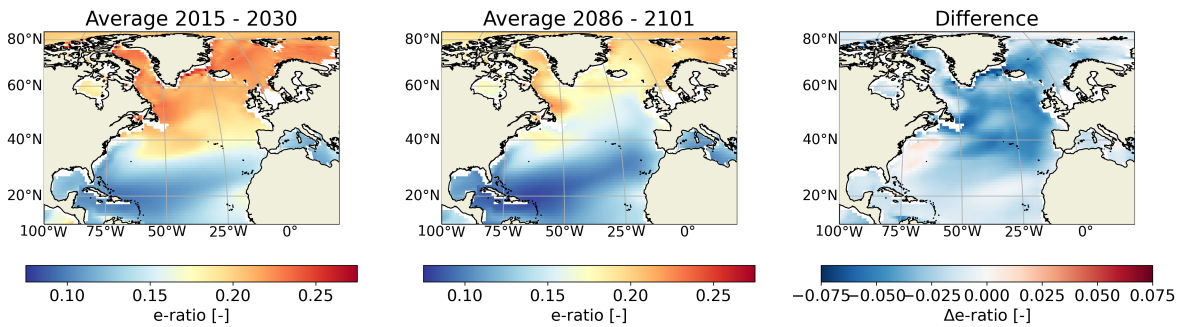

Figure S9. (a) Export production divided by Net Primary Production in the North Atlantic averaged over 2015-2030 in CESM2. (b) As in a but for the time period 2086-2101. (c) The difference between the two.

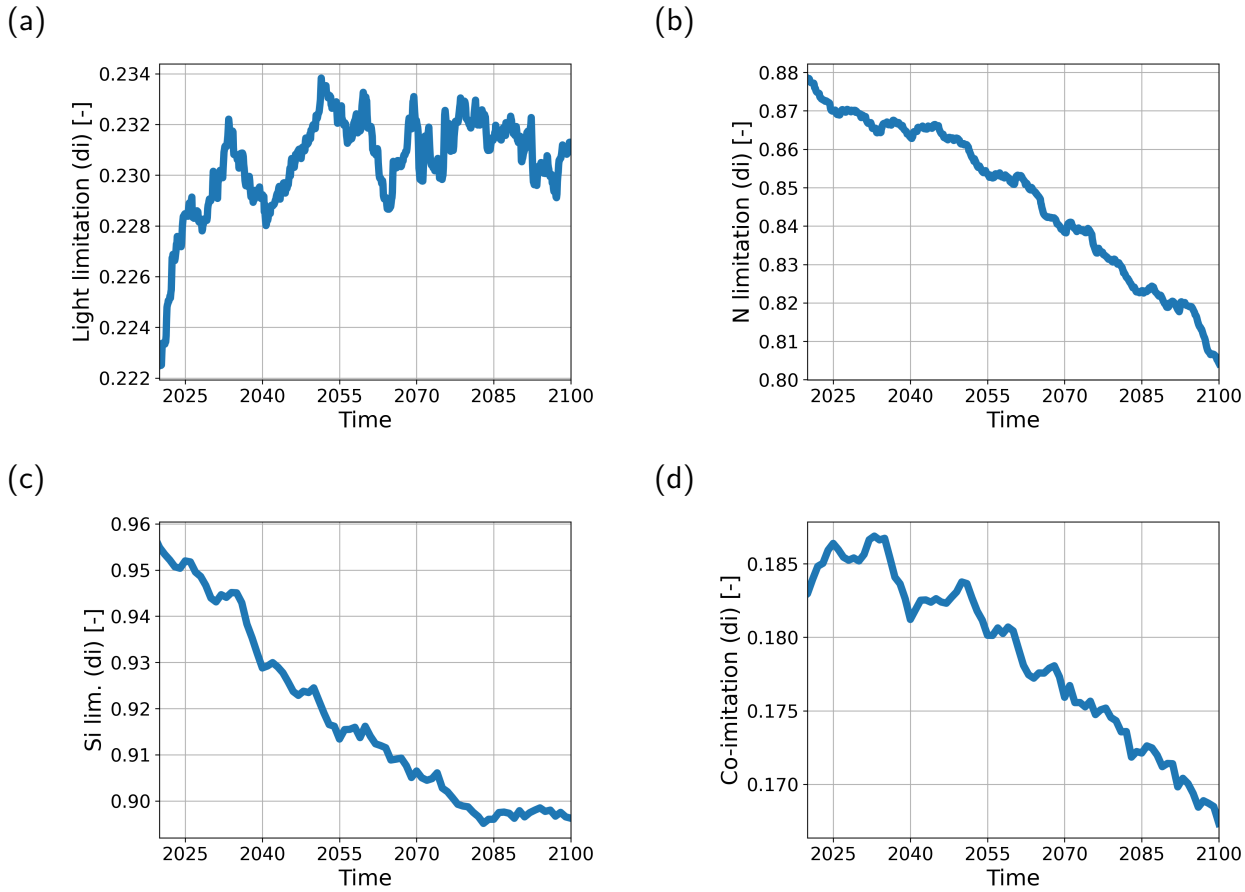

Figure S10. (a) Light limitation for diatoms in the region 45°-70°N × 270°-30°E in CESM2. Lower limitation values represent more limitation. (b) As in (a) but for nitrogen. (c) As in (a) but for silicate. (d) Nutrient-light co-limitation in the same region. Note that nitrogen is not necessarily the limiting nutrient in the entire domain for each time step. Different nutrient limitations are taken into account before averaging over mentioned region. Therefore the co-limitation is not simply the product of (a) and (b).

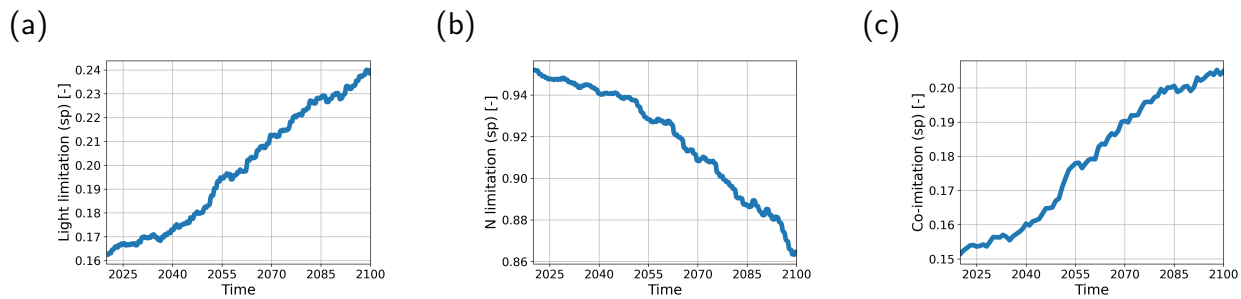

Figure S11. (a) Light limitation for small phytoplankton in the region 45°-70°N × 270°-30°E in CESM2. Lower limitation values represent more limitation. (b) As in (a) but for nitrogen. (c) Nutrient-light co-limitation in the same region. Different nutrient limitations are taken into account before averaging over mentioned region. Therefore the co-limitation is not simply the product of (a) and (b).

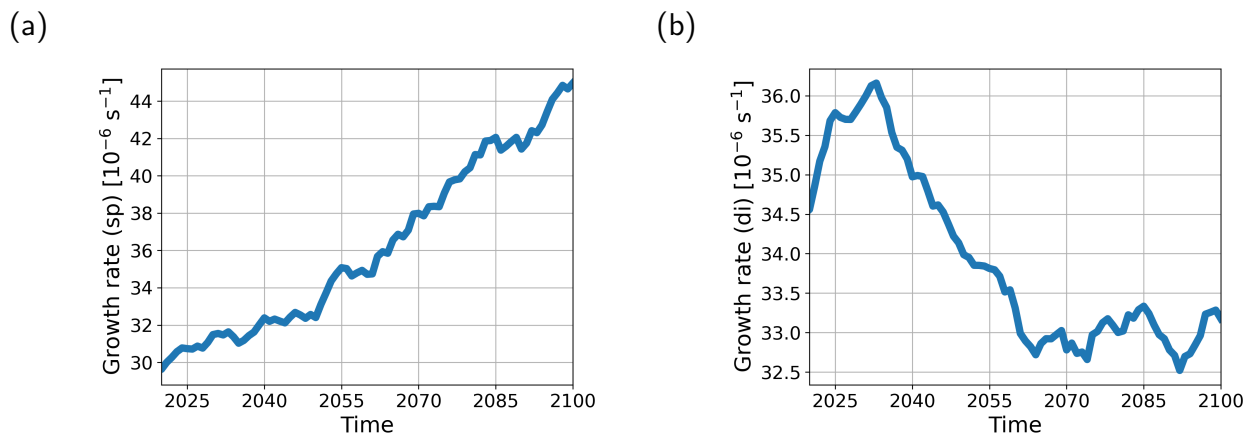

Figure S12. (a) Growth rate of small phytoplankton in 10^{-6} s^{-1} averaged over the top 100m in the region 45°-70°N × 270°-30°E in CESM2. (b) As in (a) but for diatoms.

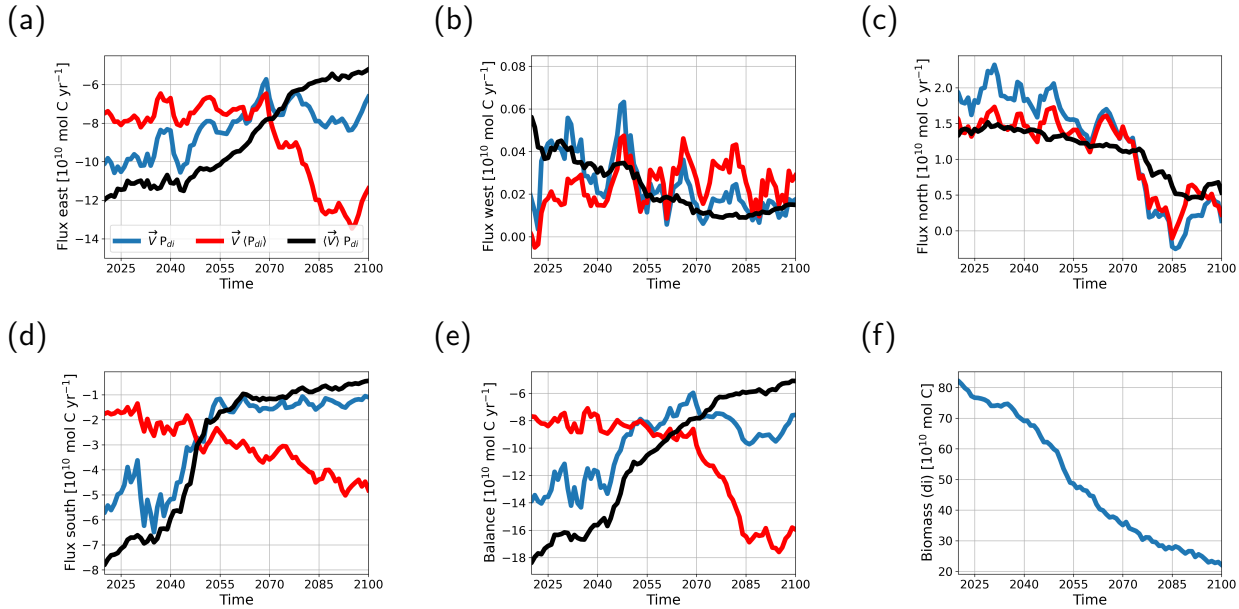

Figure S13. Advective fluxes of diatom biomass in and out of the region 45°-70°N × 270°-0°E for the top 150m of the water column for (a) the eastern boundary, (b) the western boundary, (c) the northern boundary, (d) the southern boundary, and (e) the sum of the four in CESM2. (a-d) In 10^{10} mol C yr^{-1}. (e) In 10^{10} mol C yr^{-1}. (f) The biomass content of this same region in 10^{10} mol C. Blue lines represent the actual calculated flux, red lines represent a flux where the biomass is time averaged over the entire period, and the black line a flux where the velocity field is time averaged over the entire period.

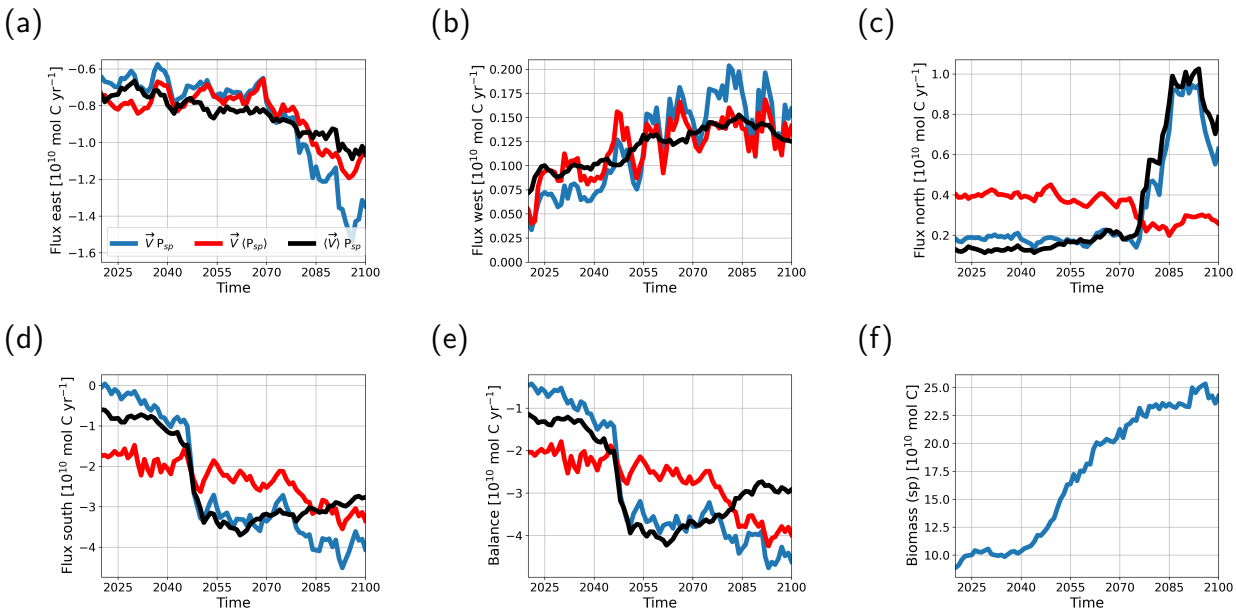

Figure S14. As in Fig. S13 but for small phytoplankton instead of diatoms.

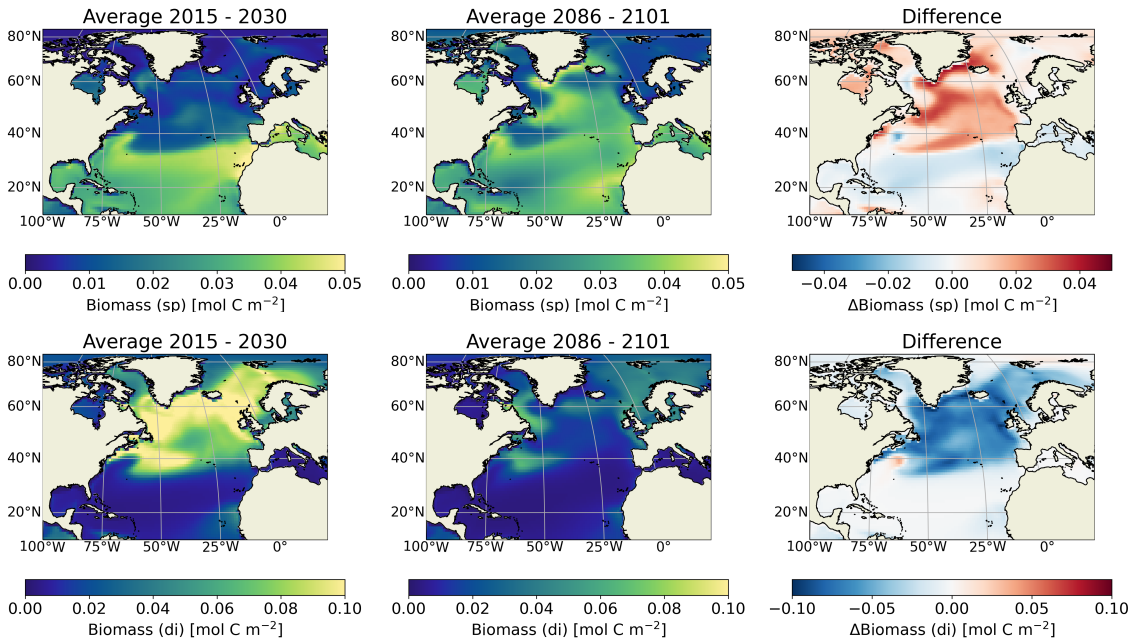

Figure S15. Phytoplankton biomass in mol C m^{-2} over the top 150 m for small phytoplankton (top row) and diatoms (bottom row) in CESM2. Note the different scaling for the diatoms. The left panels represent the average over 2015-2030, the middle panel the average over 2086-2101, and the right panel the difference between the two.